IEEE Photonics Journal
An IEEE Photonics Society Publication

Open Access

Microcavity Laser Based on Cholesteric Liquid Crystal Doped With Reactive Mesogen

Volume 8, Number 4, August 2016

Y. Li
D. Luo
R. Chen

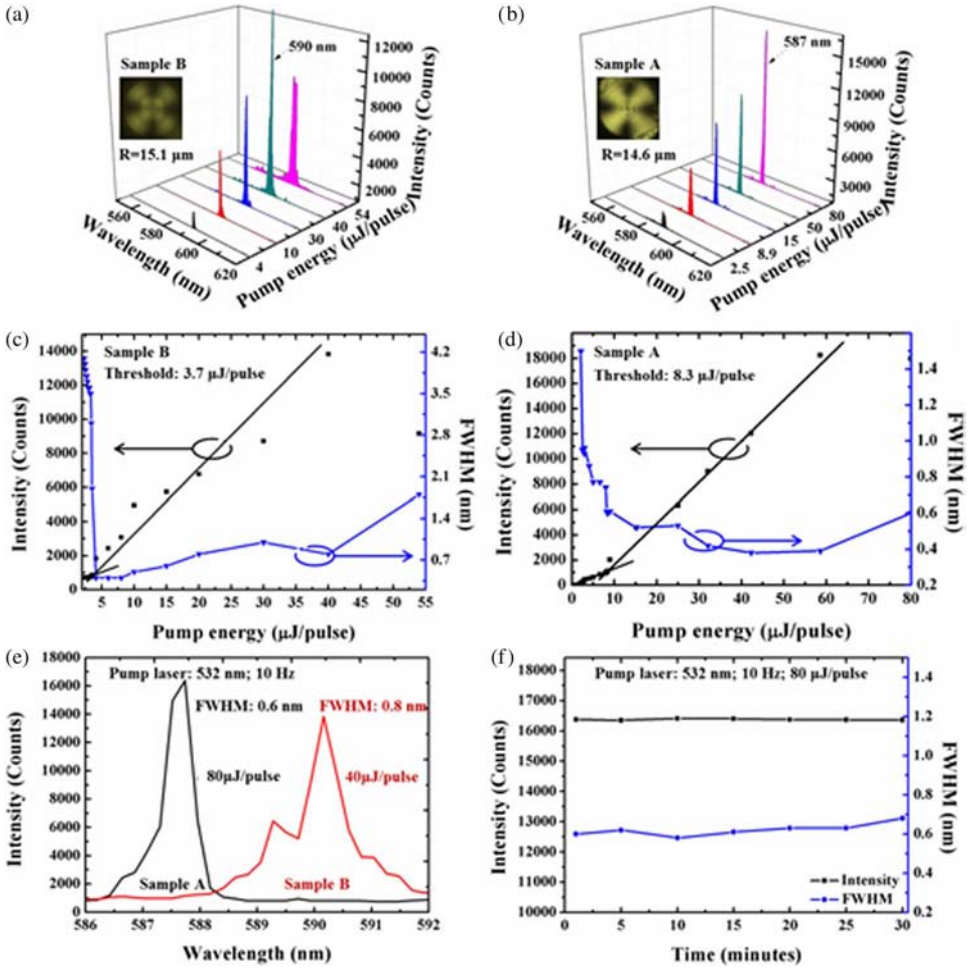

DOI: 10.1109/JPHOT.2016.2585918

IEEE photonics SOCIETY

IEEE

Microcavity Laser Based on Cholesteric Liquid Crystal Doped With Reactive Mesogen

Y. Li, D. Luo, and R. Chen

Department of Electrical and Electronic Engineering, Southern University of Science and Technology, Shenzhen 518055, China

DOI: 10.1109/JPHOT.2016.2585918

Manuscript received May 26, 2016; revised June 18, 2016; accepted June 24, 2016. Date of publication July 7, 2016; date of current version July 22, 2016. This work was supported in part by the National Natural Science Foundation of China under Grant 61405088 and Grant 11574130 and in part by the Shenzhen Science and Technology Innovation Council through the Basic Research Program under Grant JCYJ20150601155130435. Corresponding author: D. Luo (e-mail: luo.d@sustc.edu.cn).

Abstract: We demonstrate an omnidirectional laser from a 3-D Bragg microcavity, which is fabricated from a cholesteric liquid crystal that is doped with reactive mesogen. The wavelength of the laser is found to be determined by the position of the photonic band-gap that was formed within the 3-D Bragg microcavity. Compared with the laser from pure cholesteric liquid crystal microcavity, a rigid polymer network is formed within the microcavity due to the doped reactive mesogen. The polymer network successfully enhances the resistance ability of the 3-D Bragg microcavity to higher pump power by 1.5 times, thus leading to a more stable laser based on it. This laser may have potential use in optics, displays, and other photonic devices.

Index Terms: Dye laser, photonic bandgap structures.

1. Introduction

Cholesteric liquid crystals (CLCs) have attracted considerable research interests for developing various photonic devices such as electrically switchable light shutters [1]–[4], dynamic Bragg gratings [5], bi-stable reflective display devices [6], broad-band polarizers [7], and microcavity lasers [8]–[10]. The CLC molecules have a helical structure in which the director is twisted uniformly in space as a function of position along the helical axis, perpendicular to the director. The periodic variation of the refractive index generates a photonic band-gap (PBG) [7], which is sensitive to external stimulus such as mechanical stress [11], optical radiation [12], electric field [13], magnetic field, [14] and temperature [15].

An omnidirectional laser has been realized by dispersing CLC droplets with glycerol, where a 3-D Bragg optical microcavity can be formed [16]. This point-like, coherent, and omnidirectional lasing is another promising candidate for telecommunications, sensing, biomedical engineering, and display applications [16]. However, the 3-D Bragg cavity formed by pure CLC is quite easily deformed or even destroyed under high pump energy. Therefore, the real application of such an omnidirectional laser is seriously hindered by poor stability when high pump energy used. If the stability of the 3-D microcavity can be increased, the laser could resist higher pumping power without structure deformation. One possible solution is to add polymer materials.

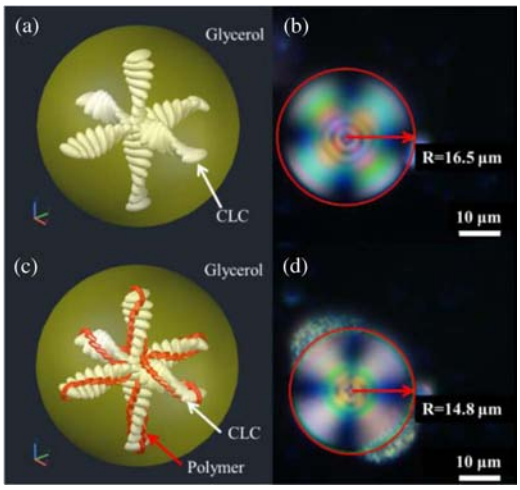

Fig. 1. Schematic configuration of the 3-D CLC Bragg microcavity (a) before polymerization and (c) after polymerization. Optical image of the 3-D CLC Bragg microcavity (b) before polymerization and (d) after polymerization. The scale bar represents 10 μm.

Reactive mesogen (RM), which is a sort of polymerizable liquid crystal, is of significant interest for a wide range of applications including blue phase template 3-D microcavity [17], engineering of retarders [18], and one-dimensional optical cavity [19], [20]. By doping RM into CLC to form 3-D microcavity, the stability of lasing could be largely increased through the formation of rigid polymer network under ultraviolet (UV) illumination.

In this paper, we report the fabrication of 3-D Bragg microcavity based on cholesteric liquid crystal and reactive mesogen. An omnidirectional laser is demonstrated and the wavelength of laser is determined by the position of photonic bandgap that formed within the 3-D Bragg microcavity. Comparing with that laser from pure CLC microcavity, a rigid polymer network is formed within the microcavity due to the doped RM. The polymer network enhances the resistance ability of the 3-D Bragg microcavity to higher pump power, thus leads to a more stable laser based on it.

2. Experimental Details

The mixture used in our experiment consists of cholesteric liquid crystals (72.15 wt%), RM (25.42 wt%), photo-initiator (1.43 wt%, Darocur1173 Sigma-Aldrich), and laser dye pyrromethene 597 (1 wt%, PM597, Exciton). The cholesteric liquid crystal was prepared by adding high twisting power chiral dopant R5011 (3.09 wt%, HCCH) into nematic liquid crystal E7 (96.91 wt%, $n_e = 1.71$ and $n_o = 1.52$, HCCH). The RM was mixed by five materials: RM257, RM82, RM006, RM021, and RM010 (all from Shijiazhuang Sdyano Fine Chemical Co., Ltd), at 30 : 15 : 20 : 20 : 15 weight ratio [21].

Then, the CLC/RM mixture was dispersed in glycerol. The weight ratio of CLC/RM mixture and glycerol was 4:96. Preparation of microcavities was conducted with a magnetic stirrer at a rotation speed of 800 rpm and rotation time of 10 minutes. Next, the microcavities in glycerol were injected by capillary action into a LC cell with gap of 150 μm, and then illuminated by an UV light (UVEC-4II, LOTS) for 15 min at power density of 15 mW/cm^2, as the sample A. For comparison purpose, microcavities based on pure CLC were prepared by similar process using laser dye PM597 doped CLC and glycerol with weight ratio of 4:96, as sample B.

Fig. 1(a) depicts the schematic configuration of 3-D Bragg microcavity from sample A (CLC/RM and glycerol) before polymerization. In glycerol, the CLC microcavities were formed naturally due to the surface tension between CLC and glycerol, where the surface tension intended to reduce the amount of surface for a given volume [16]. In CLC microcavities, the optical axis of liquid crystal molecules (white rods) twisted with a fixed angle between two adjacent

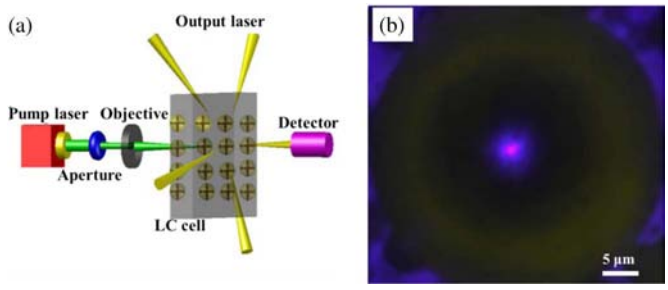

Fig. 2. (a) Schematic of optical setup for lasing. (b) Fluorescence image observed by optical microscope. The scale bar represents 5 μm.

molecules, resulting in a spiral pile structure perpendicular to the surface of microcavity. Therefore, the self-assembled 3-D Bragg microcavity with alternating high and low refractive index was formed. Fig. 1(b) demonstrates the optical image of 3-D CLC Bragg microcavity obtained under polarizing optical microscope (POM) before polymerization. The petal-like image indicates the periodic modulation of refractive index of 3-D microcavity, where several rings formed due to the spatial variation of the refractive index of in the radial direction. The radius of observed CLC microcavity is $\sim$16.5 μm.

After UV illumination, the RM monomers were polymerized within the 3-D Bragg microcavity. A simple illustration of the 3-D Bragg microcavity after polymerization is demonstrated in Fig. 1(c). The polymers (represented by the red part) adhere and strengthen the helical structure of CLC microcavity. A photograph of the CLC microcavity after polymerization obtained between crossed polarizers is presented in Fig. 1(d). Comparison with Fig. 1(b), the optical image of microcavity changes slightly. The radius of microcavity becomes smaller after polymerization (from 16.5 μm to 14.8 μm), which is probably due to the volume shrinkage resulting from the reaction of polymerization and cross linking [22]. In addition, the blue-shift of PBG in reflectance spectrum (see Fig. 3) indicates the pitch within microcavity also becomes shorter.

To generate laser, a Q-switched Neodymium-doped Yttrium Aluminum Garnet (Nd:YAG) laser with wavelength of 532 nm was used to pump the microcavity. The pulse width, repetition rate and pulse energy of Nd:YAG laser were 10 ns, 10 Hz and 40 μJ/pulse, respectively. A pump laser beam with diameter (D) of 6 mm (through an aperture) was focused by an objective (LMH-20X-532, Thorlabs) with focal length (f) of 5 mm. The beam waist (w) at the focal point was calculated by $w = \lambda/\sin\theta = 0.9$ μm, where λ is the wavelength of the pump laser and $\sin\theta \approx D/(2f) = 0.6$. A fiber-optical spectrometer (USB2000+, Ocean optics) was used to capture the spectrum of emission laser. The optical setup for lasing is shown in Fig. 2(a). Fig. 2(b) shows a fluorescence image observed by optical microscope, where the bright spot in center represents the center of CLC microcavity [16].

3. Results and Discussions

Fig. 3(a) and (b) plots the reflectance and fluorescence emission of 3D CLC Bragg microcavity in sample A before and after polymerization, respectively. From Fig. 3(a), we can see that the PBG is located from 630 nm to 702 nm with center of 668 nm. The pump energy is 40 μJ/pulse. The photoluminescence (PL) of laser dye PM597 (peaks at 582 nm) was not overlapped with both of long and short edges of PBG, marked in yellow regions. Therefore, no laser emission was generated in this case. After polymerization, the center of PBG blue-shifted from 668 nm to 564 nm. In Fig. 3(b), the photoluminescence of laser dye PM597 PL wavelength was overlapped with the long edge of PBG in reflectance spectrum, thus generating microcavity laser at wavelength of 587 nm with full width at half maximum (FWHM) of 0.4 nm. The pump energy was 70 μJ/pulse.

For comparison purpose, we measured the emission spectrum and laser properties of sample B (where the 3-D Bragg microcavity was formed on pure CLC) and sample A,

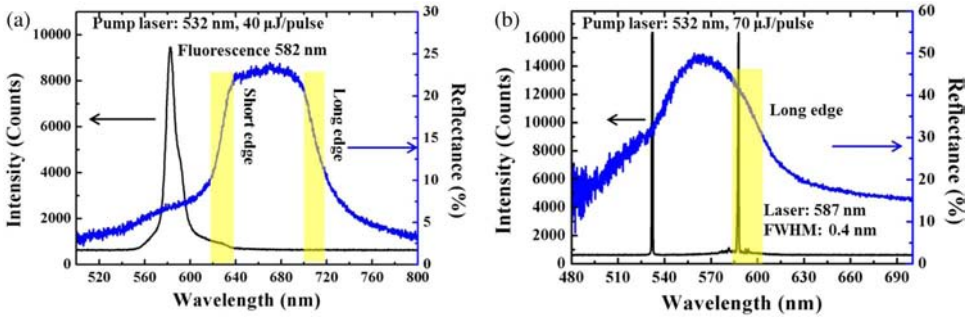

Fig. 3. Reflectance and fluorescence emission of the 3-D Bragg microcavity (a) before polymerization and (b) after polymerization.

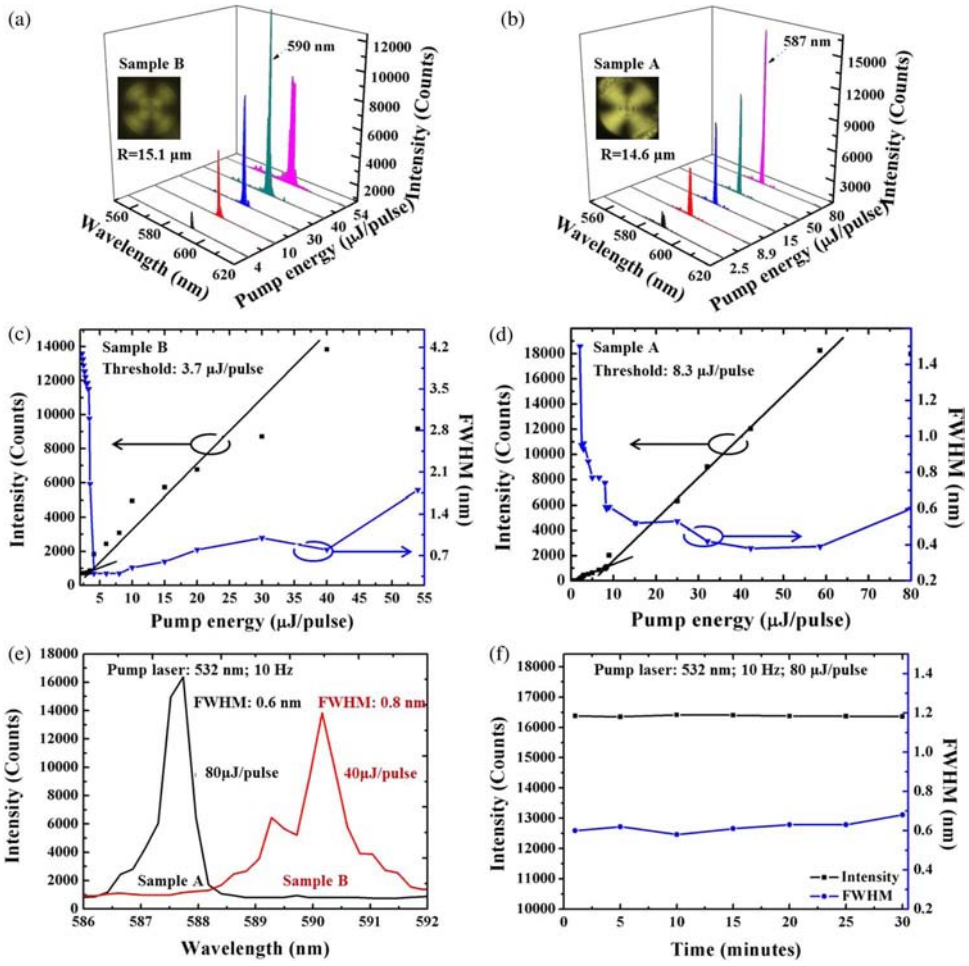

Fig. 4. Laser spectrum at different pump energies for (a) sample B and (b) sample A. Dependence of the lasing intensity and the FWHM versus the pumping energy for (c) sample B and (d) sample A. (e) Magnified and compared spectra of the FWHM for samples A and B. (f) Stability to exposing time for sample A.

respectively. Fig. 4(a) and (b) plots the evolution of the laser spectrum of sample B and sample A at different pump energies. The insets show optical images of the sample B and sample A captured by POM, where the radius of sample B and sample A is 15.1 μm and 14.6 μm,

respectively. The radius of microcavities observed here is in range of 13.5~16.5 μm. From Fig. 4(a), we can see that, the lasing (peaked at 597 nm) intensity increases with the increase of pump energy up to 54 μJ/pulse, above which the laser emission vanishes. Therefore, the damage pump energy for sample B is only 54 μJ/pulse here. In Fig. 4(b), the lasing (peaked at 587 nm) intensity increases with the increase of pump energy up to 80 μJ/pulse, which means the damage pump energy for sample A is increased up to 80 μJ/pulse and the capability of resistance to pump power is enhanced by ~1.5 times, comparing to that of sample B. Therefore, by adding RM into CLC 3-D Bragg microcavity, the damage pump energy of obtained laser can be significantly increased and the capability of resistance to pump power can be largely enhanced as well.

Fig. 4(c) and (d) depicts the dependence of lasing intensity and FWHM versus pump energy for sample B and sample A, respectively. In Fig. 4(c), the laser threshold of sample B is 3.7 μJ/pulse and the FWHM of the laser firstly reduces with the increasing pump energy to 0.4 nm and then increases when the pump energy exceeds 8 μJ/pulse. The results indicate that the stability of 3-D Bragg microcavity formed by pure CLC is quite poor. When RM is used, the poor stability of 3-D Bragg microcavity will be largely improved. In Fig. 4(d), the laser threshold of sample A is increased to 8.3 μJ/pulse. Above the threshold, the output intensity of laser increases sharply with the increase of pump energy up to 60 μJ/pulse and then saturates when the pump energy increases further to 80 μJ/pulse. In Fig. 4(e), the FWHM of sample B is 0.8 nm at pump energy of 40 μJ/pulse. In contrast, the FWHM of sample A is 0.6 nm at pump energy of 80 μJ/pulse, indicating a higher pump energy but a narrower FWHM. Therefore, the stability of lasing in sample A is much better than that in sample B. Fig. 4(f) records the dependence of lasing intensity and FWHM versus exposing time for sample A. We can see that both of intensity and FWHM of lasing are stable with pump time of 30 min and pump energy of 80 μJ/pulse.

Above experimental results indicate that the 3D microcavity of the CLC doped with RM is more stable than microcavity formed by pure CLC. For laser based on CLC microcavity with RM, the resistance ability to high pump power is largely increased from 54 μJ/pulse to 80 μJ/pulse or 1.5 times. Even the drawback is the increased threshold: from 3.7 μJ/pulse to 8.3 μJ/pulse. However, higher output intensity of laser is expected based on our proposed 3D Bragg microcavity, and this kind of omnidirectional laser with enhanced stability exhibits great application potentials in many optic and photonic fields.

4. Conclusion

In summary, we demonstrated an omnidirectional laser from 3-D Bragg microcavity based on reactive mesogen doped cholesteric liquid crystals in glycerol. The wavelength of lasing is determined by the position of photonic bandgap that formed within the 3-D Bragg microcavity. Comparing with that laser from pure CLC microcavity, a rigid polymer network is formed within the microcavity due to the doped RM. The polymer network significantly enhances the resistance ability of the 3-D Bragg microcavity to higher pump power by 1.5 times, thus leading to a more stable laser based on it. This laser may have potential use in optics, displays, and other photonic devices.

References

[1] Y. C. Hsiao, C. Y. Tang, and W. Lee, "Fast-switching bistable cholesteric intensity modulator," *Opt. Exp.*, vol. 19, no. 10, pp. 9744–9749, May 2011.
[2] P. Kumar, S. W. Kang, and S. H. Lee, "Advanced bistable cholesteric light shutter with dual frequency nematic liquid crystal," *Opt. Mater. Exp.*, vol. 2, pp. 1121–1134, 2012.
[3] H. Lu *et al.,* "Electrically switchable multi-stable cholesteric liquid crystal based on chiral ionic liquid," *Opt. Lett.*, vol. 39, no. 24, pp. 6795–6798, Dec. 2014.
[4] H. K. Bisoyi and Q. Li, "Light-directing chiral liquid crystal microcavity: From 1D to 3D," *Accounts Chem. Res.*, vol. 47, pp. 3184–3195, 2014.

[5] S. N. Lee, L. C. Chien, and S. Sprunt, "Polymer-stabilized diffraction gratings from cholesteric liquid crystals," *Appl. Phys. Lett.*, vol. 72, pp. 885–887, 1998.
[6] S. Y. Lu and L. C. Chien, "A polymer stabilized single layer color cholesteric liquid crystal display with anisotropic reflection," *Appl. Phys. Lett.*, vol. 91, 2007, Art. no. 131119.
[7] D. J. Broer, J. Lub, and G. N. Mol, "Wide-band reflective polarizers from cholesteric polymer networks with a pitch gradient," *Nature*, vol. 378, pp. 467–469, 1995.
[8] A. Muñoz *et al.,* "Continuous wave mirrorless lasing in cholesteric liquid crystals with a pitch gradient across the cell gap," *Opt. Lett.*, vol. 37, no. 14, pp. 2904–2906, Jul. 2012.
[9] Ozaki, T. Matsui, M. Ozaki, and K. Yoshino, "Electrically color-tunable defect mode lasing in one-dimensional photonic-band-gap system containing liquid crystal," *Appl. Phys. Lett.*, vol. 82, pp. 3593–3594, 2003.
[10] S. Furumi, S. Yokoyama, A. Otomo, and S. Mashiko, "Electrical control of the structure and lasing in chiral photonic band-gap liquid crystals," *Appl. Phys. Lett.*, vol. 82, pp. 16–18, 2003.
[11] G. Agez, S. Relaix, and M. Mitov, "Cholesteric liquid crystal gels with a graded mechanical stress," *Phys. Rev. E*, vol. 89, 2014, Art. no. 022513.
[12] Z. G. Zheng, Y. N. Li, H. K. Bisoyi, L. Wang, T. J. Bunning, and Q. Li, "Three-dimensional control of the helical axis of a chiral nematic liquid crystal by light," *Nature*, vol. 531, pp. 352–357, 2016.
[13] I. P. l'chishin, E. A. Tikhonov, V. G. Tishchenko, and M. Shpak, "Generation of a tunable radiation by impurity cholesteric liquid crystals," *JETP Lett.*, vol. 32, pp. 24–27, 1978.
[14] H. Coles and S. Morris, "Liquid-crystal lasers," *Nature Photon.*, vol. 4, pp. 676–685, 2010.
[15] Y. Huang, Y. Zhou, C. Doyle, and S. T. Wu, "Tuning the photonic band gap in cholesteric liquid crystals by temperature-dependent dopant solubility," *Opt. Exp.*, vol. 14, no. 3, pp. 1236–1242, Feb. 2006.
[16] M. Humar and I. Musevic, "3D microlasers from self-assembled cholesteric liquid-crystalmicrocavitys," *Opt. Exp.*, vol. 18, pp. 26995–27003, 2010.
[17] F. Castles *et al.,* "Blue-phase templated fabrication of three dimensional microcavity for photonic applications," *Nature Mater.*, vol. 11, pp. 599–603, 2012.
[18] B. Tran and T. Baur, "Reactive mesogen retarders and applications," in *Proc. SPIE Polymer Opt. Molded Glass Opt., Des., Fabrication, Mater. II*, 2012, vol. 8489, pp. 1–8.
[19] S. W. Choi *et al.,* "Photo induced circular anisotropy in a photochromic W-shaped-molecule-doped polymeric liquid crystal film," *Phys. Rev. E*, vol. 73, 2006, Art. no. 021702.
[20] M. E. McConney, V. P. Tondiglia, J. M. Hurtubise, T. J. White, and T. J. Bunning, "Photo induced hyper-reflective cholesteric liquid crystals enabled via surface initiated photo-polymerization," *Chem. Commun.*, vol. 47, pp. 505–507, 2011.
[21] Y. Li and D. Luo "Fabrication and application of 1D micro-cavity film made by cholesteric liquid crystal and reactive mesogen," *Opt. Mater. Exp.*, vol. 6, pp. 691–696, 2016.
[22] A. L. Rodarte, C. Gray, L. S. Hirst, and S. Ghosh, "Spectral and polarization modulation of quantum dot emission in a one-dimensional liquid crystal photonic cavity," *Phys. Rev. B*, vol. 85, 2012, Art. no. 035430.